AD-A264 711

DOCUMENTATION PAGE

Form Approved
OMB No. 0704-0188

2. REPORT DATE	3. REPORT TYPE AND DATES COVERED
March 1993	Professional Paper

4. TITLE AND SUBTITLE
PHOTO INDUCED CHARGE SEPARATION IN Q1D HETEROJUNCTION MATERIALS: EVIDENCE FOR ELECTRON-HOLE PAIR SEPARATION IN MIXED-HALIDE MX SOLIDS

5. FUNDING NUMBERS
In House Funding

6. AUTHOR(S)
L. A. Worl, S. C. Huckett, B. I. Swanson, A. Saxena, A. R. Bishop, J. T. Gammel

7. PERFORMING ORGANIZATION NAME(S) AND ADDRESS(ES)
Naval Command, Control and Ocean Surveillance Center (NCCOSC)
RDT&E Division
San Diego, CA 92152–5001

8. PERFORMING ORGANIZATION REPORT NUMBER

9. SPONSORING/MONITORING AGENCY NAME(S) AND ADDRESS(ES)
Naval Command, Control and Ocean Surveillance Center (NCCOSC)
RDT&E Division
San Diego, CA 92152–5001

10. SPONSORING/MONITORING AGENCY REPORT NUMBER

11. SUPPLEMENTARY NOTES

12a. DISTRIBUTION/AVAILABILITY STATEMENT
Approved for public release; distribution is unlimited.

12b. DISTRIBUTION CODE

13. ABSTRACT (Maximum 200 words)

Resonance Raman experiments on doped and photoexcited single crystals of mixed-halide MX complexes (M = Pt; X = Cl, Br) clearly indicate charge separation: electron polarons preferentially locate on PtBr segments while hole polarons are trapped within PtCl segments. This polaron selectivity, potentially very useful for device applications, is demonstrated theoretically using a discrete, 3/4-filled, two-band, tight-binding, extended Peierls-Hubbard model. Strong hybridization of the PtCl and PtBr electronic bands is the driving force for separation.

Published in *Physical Review Letters*.

14 SUBJECT TERMS		15 NUMBER OF PAGES
doped single crystals photoexcited single crystals	PtBr segments	16 PRICE CODE

17 SECURITY CLASSIFICATION OF REPORT	18 SECURITY CLASSIFICATION OF THIS PAGE	19 SECURITY CLASSIFICATION OF ABSTRACT	20 LIMITATION OF ABSTRACT
UNCLASSIFIED	UNCLASSIFIED	UNCLASSIFIED	SAME AS REPORT

21a. NAME OF RESPONSIBLE INDIVIDUAL	21b. TELEPHONE *(Include Area Code)*	21c. OFFICE SYMBOL
J. T. Gammel	(619) 553–6576	Code 573

Photoinduced charge separation in Q1D heterojunction materials: Evidence for electron-hole pair separation in mixed-halide MX solids

L.A. Worl[1], S.C. Huckett[1], B.I. Swanson[1], A. Saxena[2], A.R. Bishop[2], and J. Tinka Gammel[2,a]

[1] *Isotope and Structural Chemistry Group,*

[2] *Theoretical Division and Centers for Nonlinear Studies and Materials Science, Los Alamos National Laboratory, Los Alamos, New Mexico 87545*

Resonance Raman experiments on doped and photoexcited single crystals of mixed-halide MX complexes (M=Pt; X=Cl, Br) clearly indicate charge separation: electron polarons preferentially locate on PtBr segments while hole polarons are trapped within PtCl segments. This polaron selectivity, potentially very useful for device applications, is demonstrated theoretically using a discrete, 3/4-filled, two-band, tight-binding, extended Peierls-Hubbard model. Strong hybridization of the PtCl and PtBr electronic bands is the driving force for separation.

PACS numbers: 71.38+i, 78.30.-j, 71.10.+x

Halogen-bridged mixed-valence transition metal linear chain complexes (or MX chains) are highly anisotropic, quasi one-dimensional (Q1D) materials related to conducting polymers, mixed-stack charge-transfer salts, and oxide superconductors in terms of their low dimensionality and competing electron-phonon (e-p) and electron-electron (e-e) interactions [1]. A typical crystal consists of an array of alternating metal (M: Pt, Pd, Ni) and halogen (X: Cl, Br, I) atoms; with ligands attached to the metals, and in some cases counterions between the chains to maintain charge neutrality. Electrical conductivities range from values typical for insulators to those for small-gap semiconductors. The best studied examples of this class of Q1D materials are based on the ethylenediamine (en) complexes, $[Pt(en)_2][Pt(en)_2X_2]\cdot(ClO_4)_4$, hereafter referred to as PtX. Experimentally, this large class of single crystal materials can be systematically tuned using pressure [2], doping [3], and chemical variations of M, X, and the ligands [1] between various ground state extremes; namely from the valence-localized, strongly Peierls distorted charge-density-wave (CDW) regime (PtCl), to the valence-delocalized weak CDW regime (PtI), to the undistorted spin-density-wave (SDW) phase observed in NiBr [4]. One experimental manifestation of the tunability is absorption spectra: the intervalence charge transfer (IVCT) absorption band edge for PtCl, PtBr, and PtI occurs at $\sim$ 2.4, 1.5, and 1.0 eV, respectively. From a theoretical perspective, strong competitions for broken-symmetry ground states such as bond-order-wave (BOW), CDW, SDW, and possibly spin-Peierls in these materials are governed by *both* the e-p and e-e interactions, as well as dimensionality. Furthermore, the MX chains provide us with an opportunity to probe doping- and photo-induced local defect states [5, 6] (kinks, polarons, bipolarons, excitons) and their interactions in controlled environments for a wide

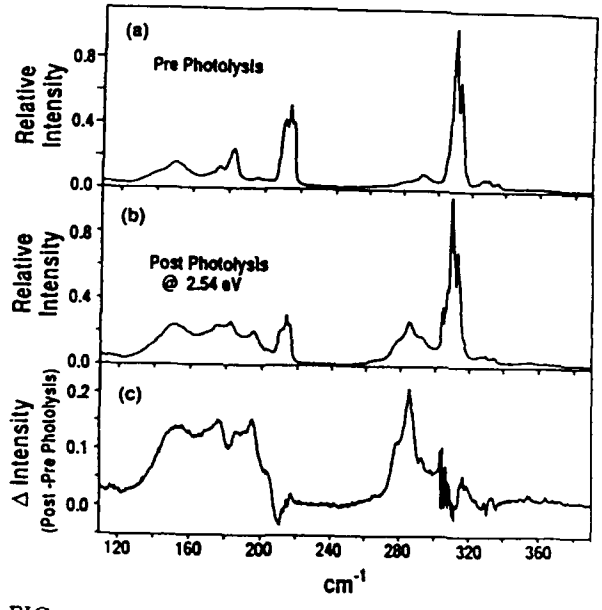

FIG. 1. Resonance Raman spectra at 1.34 eV of $PtCl_{.75}Br_{.25}$ mixed-halide crystal (a) before and (b) after photolysis with 2.54 eV excitation at 13 K. (c) Difference spectra: Post-photolysis intensity minus pre-photolysis intensity.

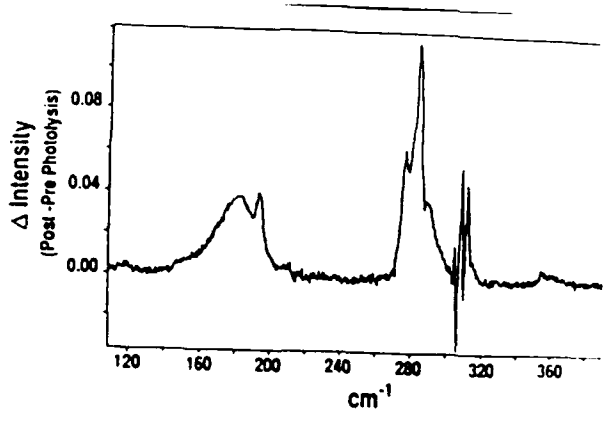

FIG. 2. Difference resonance Raman spectra at 1.34 eV of $PtCl_{.95}Br_{.05}$ mixed-halide crystal.

variety of novel ground states.

In this Letter we report an extension of our combined program on synthesis, characterization, and modeling of the MX class of materials to *mixed-halide* systems. From an experimental perspective we have obtained direct spectroscopic evidence (vibrational modes and electronic absorption) of *charge separation* in the mixed-halide systems. The electronic structure has been probed using resonance Raman (RR) excitation profiles. The spectroscopic signatures of electron (P^-) and hole (P^+) polarons in pure MX chains were reported earlier [5–8]. We recently reported the preparation of a series of $PtCl_xBr_{1-x}$ mixed-halide materials that form homogeneous crystalline solids over the entire $0< x <1$ range due to nearly identical crystal structure parameters [9]. We have also prepared mixed-halide solids consisting of $PtCl_xI_{1-x}$ and $PtBr_xI_{1-x}$, that, due to phase separations, form only in the narrow doping range near the pure PtCl, PtBr, or PtI compositions. Significantly, these mixed materials consist of segments of pure PtBr and PtCl producing interfaces (or junctions) between the two distinct halide segments. Thus, within a single $PtCl_xBr_{1-x}$ crystal there are long segments of PtCl and PtBr with spectral signatures unperturbed from the respective pure materials. This offers the opportunity to study a class of materials that contain interfaces *within a single crystal*.

Theoretically, we used a Hartree-Fock spatially inhomogeneous mean-field approximation to study the electronic structure [10], and a direct-space random phase approximation to investigate phonons [11] (and associated infrared and RR spectra) in appropriate many-body Hamiltonians. Direct comparison between experiment and theory substantiates charge separation in mixed-halide systems: electron polarons locate in the PtBr segment while hole polarons locate in the PtCl segment of a $PtCl_xBr_{1-x}$ chain. Though we only report here on the PtCl/PtBr system, we find polaronic selectivity for all Pt-based mixed-halide systems (Cl/Br, Br/I, and Cl/I). From a band structure point of view, mixed-halide chains represent a 1D analog of heterojunctions in semiconductors. In this context, we emphasize that the charge separation is a nontrivial result of *strong* lattice relaxation and not simply undoped band structure considerations.

Synthesis of pure PtCl, pure PtBr, and mixed PtCl/PtBr solids are described elsewhere [9, 12]. Composition was determined by ^{1}H NMR as described previously [9]. In all cases a crystal was divided and one portion used for Raman measurements and the other for ^{1}H NMR analysis. Raman spectra were obtained from single crystals at 13±2 K with incident intensities less than 2 mW. The tunable red/near-infrared and visible RR excitation instruments have previously been described [6]. Both incident and scattered light were polarized parallel to the chain axis. For photolysis, the 488 nm line of the Ar^+ ion laser was defocused on the crystal for 1-1.5 hours. Photolytic incident intensities were 2 mW.

Upon photolysis of mixed-halide materials, photoinduced charged defects are produced in high concentration and become preferentially located on particular chain segments. In Figs. 1(a) and 1(b), the RR spectrum probed at 1.34 eV of a mixed $PtCl_{.75}Br_{.25}$ crystal is shown before and after photolysis at 2.54 eV (beyond the band edge of pure PtCl). Fig. 1(c) illustrates the difference spectrum between pre- and post-photolysis results. This is an excitation energy (1.34 eV) where resonance enhancement is known to occur for the P^+ and P^- in PtCl, and a region of pre-resonance for the electron bipolaron and P^- in PtBr. As shown in Fig. 1(a), prior to photolysis the Cl–Pt'^{V}–Cl symmetric stretch chain mode at 308 cm^{-1} dominates the spectra. Weak features at ~285 and 325 cm^{-1} are attributed to P^- defects and edge state modes in PtCl segments, respectively. In the spectral region for PtBr, modes at 213 and 181 cm^{-1} are observed which are vibrational signatures for PtBr edge states. (Our calculations yield an edge mode at ~210 cm^{-1} for a Cl–Pt'^{V}–Br interface.) Also observed are relatively weak features at 196, 174, and 150 cm^{-1}. The broad feature at 150 cm^{-1} has been ascribed to a P^- in a PtBr segment [7]. The distinct features between 181 and 171 cm^{-1} modes are attributed to the Br–Pt'^{V}–Br symmetric stretch for short correlation length chain segments [13]. The characteristic chain mode observed in pure PtBr (166 cm^{-1}) is not seen, indicating that long Br segments (≥10 PtBr) are not present in the material.

Photolysis within the band gap of PtCl and in the ultragap region of PtBr (2.54 eV) causes an increase in P^+ defects localized within the PtCl segments at ~285 cm^{-1} [Figs. 1(b) and 1(c)]. These results are in contrast to the photolysis of pure materials: in pure crystals of PtCl, RR studies show an increase in *both* P^- (263 cm^{-1}) and P^+ (287 cm^{-1}) local modes. Significantly, in the mixed materials, *no* P^- features appear in the PtCl segments with photolysis. In the PtBr segments, the P^- defect at 150 cm^{-1} also increases in intensity. Within this region, a general increase in intensity is observed for features from 196-174 cm^{-1}. The characteristic features associated with the PtBr symmetric stretch from different chain lengths are unresolved and complicated. A further observation is that the edge state modes at ~210 and 181 cm^{-1} decrease in intensity, indicating there is a loss of unperturbed edge state.

In a second experiment, photolysis was done on a mixed crystal of $PtCl_{.95}Br_{.05}$ (Fig. 2). This material exhibited similar results within the PtCl regions: the growth of the P^+ features (~285 cm^{-1}) occurred after photolysis. Within the PtBr regions, one broad feature at 180 cm^{-1} and one sharp feature at 191 cm^{-1} increase in intensity. These features are consistent with the 25% PtBr mixed crystal, yet no features at 150 cm^{-1} are observed. Knowing these 5% PtBr photolysis results, three features are now apparent within the 196-150 cm^{-1} region for the 25% PtBr crystal [Fig. 1(c)]: two broad features at 150 and 180 cm^{-1}, and one sharp feature at 191

cm^{-1}. The 150 cm^{-1} feature arises from a P^- within PtBr segments, observed in these mixed crystals only when PtBr correlation lengths are fairly long [7]. The features at 180 and 196 cm^{-1} that grow in upon photolysis are due to an electron defect pinned at a Cl−Pt'^{V}−Br edge [13]. This creates a loss of Cl−Pt'^{V}−Br edge character and a decrease in the 181 and 210 cm^{-1} features observed in Fig. 1(c).

We studied the photoinduced defects of mixed PtCl/PtBr materials with varying stoichiometries. In *all cases* we observed selective localization of hole defects with *no* growth of electron features in PtCl segments. We further have discrete evidence for the formation of electron defects in PtBr segments. PtCl/PtI mixed materials also generate stable charge defects, yet after photolysis in these systems, there is a dramatic increase in the P^- defects in PtCl segments. This result indicates that the nature of charge separated state (electrons localized in a weak CDW and holes localized in a strong CDW) can not be predicted from the strength of CDW but must be due to other effects, such as selective excitation energies.

Turning to our theoretical modeling, we consider an isolated mixed-halide chain in which we replace a segment, containing m X atoms, by m X′ atoms where X,X′=Cl, Br. Focusing on the metal d_{z^2} and halogen p_z orbitals and including only the nearest neighbor interactions we construct the following *two band* tight-binding many-body Hamiltonian [10]:

$$H = \sum_{l\sigma}(-t_0 + \alpha\Delta_l)(c^\dagger_{l\sigma}c_{l+1\sigma} + c^\dagger_{l+1\sigma}c_{l\sigma}) + \sum_{l\sigma}[\epsilon_l - \beta_l(\Delta_l + \Delta_{l-1})]c^\dagger_{l\sigma}c_{l\sigma} + \sum_l U_l n_{l\uparrow}n_{l\downarrow} + \frac{1}{2}\sum_l K_l\Delta_l^2 + \frac{1}{2}\sum_l K^l_{MM}(\Delta_{2l} + \Delta_{2l+1})^2 , \quad (1)$$

where $c^\dagger_{l\sigma}$ ($c_{l\sigma}$) denotes the creation (annihilation) operator for the electronic orbital at the lth atom with spin σ. M and X (or X′) occupy even and odd sites, respectively. $\Delta_l := \hat{y}_{l+1} - \hat{y}_l$, where $\hat{y}_l$ are the displacements from uniform lattice spacing of the atoms at site l. Eq. (1) includes as parameters the on-site energy or electron affinity ϵ_l ($\epsilon_M = e_0$, $\epsilon_X = -e_0$, $\epsilon_{X'} = e_0 - 2e'_0$), electron hopping ($t_0, t'_0$), on-site ($\beta_M, \beta_X, \beta'_X$) and inter-site ($\alpha, \alpha'$) e-p coupling, on-site e-e repulsion (U_M, U_X, U'_X), and finally effective M-X (K) or M-X′ (K') and M-M (K_{MM}, K'_{MM}) springs to model the elements of the structure not explicitly included. In particular, K_{MM} and K'_{MM} account for the (halide-dependant) rigidity of the metal sublattice connected into a 3-dimensional network via ligands. Periodic boundary conditions were employed. Long-range Coulomb fields are also included when necessary. At stoichiometry there are 6 electrons per M_2X_2 (or $M_2X'_2$) unit, or 3/4 band filling. Note the metal M=Pt energies ϵ_{2l} are the same in both segments. The interface (edge) between the two segments can be of two types: (1) centered on a reduced metal site (Pt^{II}, the long-long bond) or (2) centered on an oxidized metal site (Pt'^{V}, the short-short bond). The corresponding electronic and phonon spectra, and thus the associated optical and Raman spectra, differ for the two cases, though the general features of charge separation are unaltered. Below we consider case (1) only. A combination of ground state experimental data and quantum chemical and band structure calculations have lead us to the effective parameter sets for the Hamiltonian, Eq. (1), listed in Table I [10].

Fig. 3(a) shows a typical mixed-halide chain considered in our numerical simulations. It contains 24 Pt and 24 halogens, with a segment containing 8 Cl replaced by 8 Br. The electronic wavefunctions and spectra (not shown here) indicate that the PtCl and PtBr bands are strongly hybridized. The highest occupied level (36) and the lowest unoccupied level (37) are PtBr-like. Therefore, one might naively expect doping- and photo-induced electrons as well as holes to locate on PtBr segment.

However, the situation changes dramatically upon doping. The electronic spectrum in the presence of a P^- is similar to the undoped chain except that the P^- levels (36, 37) move into the gap, retaining their predominantly PtBr character. Thus a P^- locates on the PtBr segment, consistent with experimental observation. For the electronic spectrum in the presence of a $P^+_\uparrow$, we find the wavefunction $\psi^{36}_\uparrow$ is still Br-like (though now unoccupied), but $\psi^{36}_\uparrow$ is no longer PtBr-like. Instead it becomes PtCl-like, as evidenced in Fig. 3(b). Note the energies, $E^{36}_\uparrow$ and $E^{36}_\downarrow$, split, as shown in Fig. 3(c), with $E^{36}_\uparrow$ and $E^{37}_\downarrow$ becoming nearly degenerate, due to the presence of a Hubbard term (U) in the Hamiltonian Eq. (1). This conversion of a PtBr-like level into a predominantly PtCl-like level subsequent to doping is a direct consequence of strong lattice relaxation in the mixed-halide systems. In other words, the strong hybridization of PtCl and PtBr levels is nontrivially affected when a charge (polaron) is added to the system. Such a strong lattice relaxation effects are unusual for conventional semiconductors and many other narrow gap materials.

To further illustrate charge separation we systematically studied the lattice relaxation. Upon doping, if we initially placed a P^- in the PtCl segment (*i.e.*, the "wrong" segment) and allowed the system to self-consistently evolve to the minimum energy configuration, we found the P^- migrated to a Pt'^{V} site in the PtBr segment. A P^+ placed in the PtBr segment migrated to a Pt^{II} site in the PtCl segment [14]. Analogously, the photogenerated exciton was invariably unstable and broke into a P^+ and a P^-, the P^+ migrating to the PtCl segment and its companion P^- to the PtBr segment [15]. These cases are illustrated in Fig. 4. Both doping and photoexcitation lead to charge separation with a specific polaron charge selectivity consistent with experimental observations.

In conclusion, we have clearly demonstrated the existence of charge separation in mixed halide systems (with PtCl/PtBr as an example) both experimentally and in

theoretical calculations. In particular the doping- and photo-induced, charged, polaronic defects preferentially locate on one part of the chain, say on MX′, rather than on MX. This selectivity and charge storage depend on the nature of the polaronic excitations as well as the choice of X and X′. Certain excitations (such as kink solitons), however, show a tendency for pinning at or in the vicinity of the interface between MX and MX′. Moreover, the halogen atoms at the edge are involved in charge transfer across the edge, and the MX unit adjacent to the edge is polarized, with distinctive local infrared and Raman "edge" modes. Thus, the mixed-halide systems are of significant interest in utilizing charge separation in potential photovoltaic or photoconductive device applications. To further our understanding in this regard we are also beginning to explore mixed-metal (e.g. PtBr/PdBr) and MMX systems.

We acknowledge fruitful discussions with R.J. Donohoe and X.Z. Huang. This work was supported by the US DOE. JTG holds a NRC-NOSC Research Associateship.

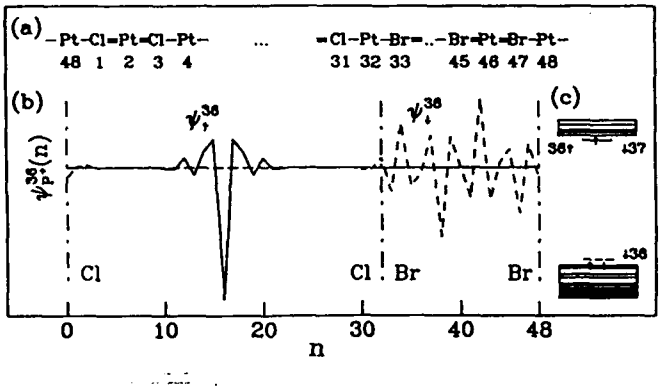

FIG. 3. (a) A PtCl chain containing a segment of PtBr. Note that both edges of the segment are Pt^{II} sites. (b) Electronic up (—) and down (---) spin wavefunctions at the Fermi surface (level 36). (c) Localized electronic levels for $P_\uparrow^+$.

FIG. 4. Excess charge (—) and spin (---) densities with respect to the mixed-chain ground state showing polaron migration for (a) $P_\uparrow^-$ and (b) $P_\downarrow^+$ on a 16 PtCl and 8 PtBr unit chain, and (c) subsequent to photoexcitation of an up spin electron between levels 36 and 37 on an 8 PtCl and 16 PtBr unit chain. The large circles indicate initial defect location, though the result is insensitive to initial condition [14, 15].

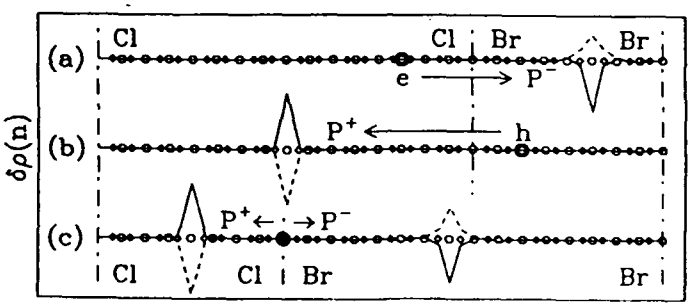

[a] Present address: Code 573, Materials Research Branch, Naval Ocean Systems Center, San Diego, CA 92152-5000.

[1] H.J. Keller, in *Extended Linear Chain Compounds*, edited by J.S. Miller (Plenum, New York, 1982), p. 357, and references therein.
[2] N. Kuroda, M. Sakai, Y. Nishina, M. Tanaka, and S. Kurita, Phys. Rev. Lett. **58**, 2122 (1987).
[3] M. Haruki and S. Kurita, Phys. Rev. B **39**, 5706 (1989).
[4] K. Toriumi, Y. Wada, T. Mitani, S. Bandow, M. Yamashita, and Y. Fujii, J. Am. Chem. Soc. **111**, 2341 (1989).
[5] S. Kurita, M. Haruki, and K. Miyagawa, J. Phys. Soc. Jpn. **57**, 1789 (1988); S. Kurita and M. Haruki, Synth. Met. **29**, F129 (1989).
[6] R.J. Donohoe, S.A. Ekberg, C.D. Tait, and B.I. Swanson, Solid State Commun. **71**, 49 (1989); R.J. Donohoe, R.B. Dyer, and B.I. Swanson, Solid State Commun. **73**, 521 (1990).
[7] R.J. Donohoe, L.A. Worl, C.A. Arrington, A. Bulou, and B.I. Swanson, Phys. Rev. B, unpublished.
[8] M. Haruki and P. Wachter, Phys. Rev. B (RC) 1991.
[9] S.C. Huckett, R.J. Donohoe, L.A. Worl, A.D.F. Bulou, C.J. Burns, J.R. Laia, D. Carroll, and B.I. Swanson, Chem. Mater. **3**, 123 (1991).
[10] J.T. Gammel, A. Saxena, I. Batistic, A.R. Bishop, and S.R. Phillpot, Phys. Rev. B (1992) in press, and references therein.
[11] I. Batistic and A.R. Bishop, Phys. Rev. B (1991).
[12] O. Bekaroglu, H. Breer, H. Endres, H.J. Keller, and H. Nam Gung, Inorg. Chim. Acta **21** 183, (1977).
[13] X.Z. Huang, L.A. Worl, A. Saxena, A.R. Bishop, and B.I. Swanson, unpublished.
[14] Local energy minima are occasionally found where the P^+ localizes in the PtBr segment. The presence and location of such metastable configurations depend on the length of both segments.
[15] No metastable minima are found in photoexcitation since P^- and P^+ repel due to strong lattice relaxation.

TABLE I. Parameters for the PtX materials in Eq. (1). E_g is the IVCT band edge, and $\beta_X = -0.5\beta_M$.

MX	Δ(Å)	E_g(eV)	t_0(eV)	α(eV/Å)	e_0(eV)	β_M(eV/Å)	U_M(eV)	U_X(eV)	K(eV/Å^2)	K_{MM}(eV/Å^2)
PtCl	0.38	2.50	1.02	0.5	2.12	2.7	1.9	1.3	6.800	0.0
PtBr	0.24	1.56	1.26	0.7	0.60	1.8	0.0	0.0	6.125	0.7